

Holographic dark energy models: A comparison from the latest observational data

Miao Li,^{1,2,*} Xiao-Dong Li,^{3,1,†} Shuang Wang,^{4,1,‡} and Xin Zhang^{5,2,§}

¹*Institute of Theoretical Physics, Chinese Academy of Science, Beijing 100080, China*

²*Kavli Institute for Theoretical Physics China,
Chinese Academy of Sciences, Beijing 100080, China*

³*Interdisciplinary Center for Theoretical Study,
University of Science and Technology of China, Hefei 230026, China*

⁴*Department of Modern Physics, University of Science and Technology of China, Hefei 230026, China*

⁵*Department of Physics, College of Sciences,
Northeastern University, Shenyang 110004, China*

The holographic principle of quantum gravity theory has been applied to the dark energy (DE) problem, and so far three holographic DE models have been proposed: the original holographic dark energy (HDE) model, the agegraphic dark energy (ADE) model, and the holographic Ricci dark energy (RDE) model. In this work, we perform the best-fit analysis on these three models, by using the latest observational data including the Union+CFA3 sample of 397 Type Ia supernovae (SNIa), the shift parameter of the cosmic microwave background (CMB) given by the five-year Wilkinson Microwave Anisotropy Probe (WMAP5) observations, and the baryon acoustic oscillation (BAO) measurement from the Sloan Digital Sky Survey (SDSS). The analysis shows that for HDE, $\chi^2_{min} = 465.912$; for RDE, $\chi^2_{min} = 483.130$; for ADE, $\chi^2_{min} = 481.694$. Among these models, HDE model can give the smallest χ^2_{min} . Besides, we also use the Bayesian evidence (BE) as a model selection criterion to make a comparison. It is found that for HDE, ADE, and RDE, $\Delta \ln BE = -0.86$, -5.17 , and -8.14 , respectively. So, it seems that the HDE model is more favored by the observational data.

PACS numbers: 98.80.-k, 95.36.+x

I. INTRODUCTION

Observations of Type Ia supernovae (SNIa) [1], cosmic microwave background (CMB) [2] and large scale structure (LSS) [3] all indicate the existence of mysterious dark energy (DE) driving the current accelerating expansion of the universe. The most obvious theoretical candidate of dark energy is the cosmological

*Electronic address: mli@itp.ac.cn

†Electronic address: renzhe@mail.ustc.edu.cn

‡Electronic address: swang@mail.ustc.edu.cn

§Electronic address: zhangxin@mail.neu.edu.cn

constant Λ , which can fit the observations well, but is plagued with the fine-tuning problem and the coincidence problem [4]. Numerous other dynamical DE models have also been proposed in the literature, such as quintessence [5], phantom [6], k -essence [7], tachyon [8], hessence [9], Chaplygin gas [10], Yang-Mills condensate [11], ect.

Actually, the DE problem may be in essence an issue of quantum gravity [12]. However, by far, a complete theory of quantum gravity has not been established, so it seems that we have to consider the effects of gravity in some effective field theory in which some fundamental principles of quantum gravity should be taken into account. It is commonly believed that the holographic principle [13] is just a fundamental principle of quantum gravity. Based on the effective quantum field theory, Cohen et al. [14] pointed out that the quantum zero-point energy of a system with size L should not exceed the mass of a black hole with the same size, i.e. $L^3\rho_{vac} \leq LM_{Pl}^2$, where ρ_{vac} is the quantum zero-point energy density, and $M_{Pl} \equiv 1/\sqrt{8\pi G}$ is the reduced Planck mass. This observation relates the ultraviolet (UV) cutoff of a system to its infrared (IR) cutoff. When we take the whole universe into account, the vacuum energy related to this holographic principle can be viewed as dark energy (its energy density is denoted as ρ_{de} hereafter). The largest IR cutoff L is chosen by saturating the inequality, so that we get the holographic dark energy density

$$\rho_{de} = 3c^2 M_{Pl}^2 L^{-2}, \quad (1)$$

where c is a numerical constant characterizing all of the uncertainties of the theory, and its value can only be determined by observations. If we take L as the size of the current universe, for instance the Hubble radius H^{-1} , then the dark energy density will be close to the observational result. However, Hsu [15] pointed out this yields a wrong equation of state (EOS) for DE.

Li [16] suggested to choose the future event horizon of the universe as the IR cutoff. This is the original holographic dark energy model. Subsequently, Cai proposed [17] that the age of the universe can be chosen as the IR cutoff, and this model is called agegraphic dark energy model. A new version of this model replacing the age of the universe by the conformal age of the universe was also discussed [18], in order to avoid some internal inconsistencies in the original model. Furthermore, Gao et al. [19] proposed to consider the average radius of the Ricci scalar curvature as the IR cutoff, and this model is called holographic Ricci dark energy model. (For convenience, hereafter we will call them HDE, ADE, and RDE, respectively.) Although these three models have been studied widely [20, 21, 22], so far no comparison of them has been made. It would be very interesting to constrain the holographic dark energy models by using the latest observational data, and then make a comparison for them by using the proper model selection criterion. This will be done in this work.

This paper is organized as follows: In Section 2, we briefly review the holographic DE models. In

Section 3, we present the method of data analysis, as well as the model selection criterion. In Section 4, we show the results of the cosmological constraints, and we also use the Bayesian evidence (BE) to make a comparison. Section 5 is a short summary. In this work, we assume today's scale factor $a_0 = 1$, so the redshift z satisfies $z = a^{-1} - 1$; the subscript "0" always indicates the present value of the corresponding quantity, and the unit with $c = \hbar = 1$ is used.

II. MODELS

In this section, we shall briefly review the holographic DE models. For a spatially flat (the assumption of flatness is motivated by the inflation scenario) Friedmann-Robertson-Walker (FRW) universe with matter component ρ_m and dark energy component ρ_{de} , the Friedmann equation reads

$$3M_{pl}^2 H^2 = \rho_m + \rho_{de} , \quad (2)$$

or equivalently,

$$E(z) \equiv \frac{H(z)}{H_0} = \left(\frac{\Omega_{m0}(1+z)^3}{1 - \Omega_{de}} \right)^{1/2} , \quad (3)$$

where $H \equiv \dot{a}/a$ is the Hubble parameter, Ω_{m0} is the present fractional matter density, and $\Omega_{de} \equiv \frac{\rho_{de}}{\rho_c} = \frac{\rho_{de}}{3M_{pl}^2 H^2}$ is the fractional dark energy density. In this work, for simplicity, we shall not discuss the issue of interaction between dark matter and dark energy, so we have

$$\dot{\rho}_m + 3H\rho_m = 0 , \quad (4)$$

$$\dot{\rho}_{de} + 3H(1 + w_{de})\rho_{de} = 0 , \quad (5)$$

where the over dot denotes the derivative with respect to the cosmic time t , and w_{de} is the EOS of DE.

A. The HDE model

For this model, the IR cutoff is chosen as the future event horizon of the universe,

$$L = a \int_t^\infty \frac{dt'}{a} = a \int_a^\infty \frac{da'}{Ha'^2} . \quad (6)$$

Taking derivative for Eq. (1) with respect to $x = \ln a$ and making use of Eq. (6), we get

$$\rho'_{de} \equiv \frac{d\rho_{de}}{dx} = 2\rho_{de} \left(\frac{\sqrt{\Omega_{de}}}{c} - 1 \right) . \quad (7)$$

Combining Eqs. (5) and (7), we obtain the EOS for HDE,

$$w_{de} = -\frac{1}{3} - \frac{2}{3c} \sqrt{\Omega_{de}}. \quad (8)$$

Directly taking derivative for $\Omega_{de} = c^2/(H^2 L^2)$, and using Eq. (6), we get

$$\Omega'_{de} = 2\Omega_{de} \left(\epsilon - 1 + \frac{\sqrt{\Omega_{de}}}{c} \right), \quad (9)$$

where $\epsilon \equiv -\dot{H}/H^2 = -H'/H$. From Eqs. (2), (4), (5), and (8), we have

$$\epsilon = \frac{3}{2}(1 + w_{de}\Omega_{de}) = \frac{3}{2} - \frac{\Omega_{de}}{2} - \frac{\Omega_{de}^{3/2}}{c}, \quad (10)$$

for this case. So, we have the equation of motion, a differential equation, for Ω_{de} ,

$$\Omega'_{de} = \Omega_{de}(1 - \Omega_{de}) \left(1 + \frac{2}{c} \sqrt{\Omega_{de}} \right). \quad (11)$$

Since $\frac{d}{dx} = -(1+z)\frac{d}{dz}$, we get

$$\frac{d\Omega_{de}}{dz} = -(1+z)^{-1} \Omega_{de}(1 - \Omega_{de}) \left(1 + \frac{2}{c} \sqrt{\Omega_{de}} \right). \quad (12)$$

Solving numerically Eq. (12) and substituting the corresponding results into Eq. (3), the key function $E(z)$ can be obtained. It should be mentioned that there are two model parameters, Ω_{m0} and c , in the HDE model.

B. The ADE model

Since there are some internal inconsistencies in the original ADE model, we will discuss the new version of ADE model which suggests to choose the conformal age of the universe

$$\eta \equiv \int \frac{dt}{a} = \int \frac{da}{a^2 H}, \quad (13)$$

as the IR cutoff, so the density of ADE is

$$\rho_{de} = 3n^2 M_{Pl}^2 \eta^{-2}. \quad (14)$$

To distinguish from the HDE model, a new constant parameter n is used to replace the old parameter c .

Taking derivative for Eq. (14) with respect to x and making use of Eq. (13), we get

$$\rho'_{de} = -2\rho_{de} \frac{\sqrt{\Omega_{de}}}{na}. \quad (15)$$

This means that the EOS of ADE is

$$w_{de} = -1 + \frac{2}{3n} \frac{\sqrt{\Omega_{de}}}{a}. \quad (16)$$

Taking derivative for $\Omega_{de} = n^2/(H^2\eta^2)$, and considering Eq. (13), we obtain

$$\Omega'_{de} = 2\Omega_{de} \left(\epsilon - \frac{\sqrt{\Omega_{de}}}{na} \right). \quad (17)$$

In this case, we have

$$\epsilon = \frac{3}{2}(1 + w_{de}\Omega_{de}) = \frac{3}{2} - \frac{3}{2}\Omega_{de} + \frac{\Omega_{de}^{3/2}}{na}. \quad (18)$$

Hence, we get the equation of motion for Ω_{de} ,

$$\Omega'_{de} = \Omega_{de}(1 - \Omega_{de}) \left(3 - \frac{2}{n} \frac{\sqrt{\Omega_{de}}}{a} \right), \quad (19)$$

and this equation can be rewritten as

$$\frac{d\Omega_{de}}{dz} = -\Omega_{de}(1 - \Omega_{de}) \left(3(1 + z)^{-1} - \frac{2}{n} \sqrt{\Omega_{de}} \right). \quad (20)$$

As in [18], we choose the initial condition, $\Omega_{de}(z_{ini}) = n^2(1 + z_{ini})^{-2}/4$, at $z_{ini} = 2000$, then Eq. (20) can be numerically solved. Substituting the results of Eq. (20) into Eq. (3), the key function $E(z)$ can be obtained. Notice that once n is given, $\Omega_{m0} = 1 - \Omega_{de}(z = 0)$ can be naturally obtained by solving Eq.(20), so the ADE model is a single-parameter model.

C. The RDE model

For a spatially flat FRW universe, the Ricci scalar is

$$\mathcal{R} = -6(\dot{H} + 2H^2). \quad (21)$$

As suggested by Gao et al. [19], the energy density of DE is

$$\rho_{de} = \frac{3\alpha}{8\pi G} (\dot{H} + 2H^2) = -\frac{\alpha}{16\pi G} \mathcal{R}, \quad (22)$$

where α is a positive numerical constant to be determined by observations. Comparing to Eq. (1), it is seen that if we identify the IR cutoff L with $-\mathcal{R}/6$, we have $\alpha = c^2$. As pointed out by Cai et al. [23], the RDE can be viewed as originated from taking the causal connection scale as the IR cutoff in the holographic setting.

Now the Friedmann equation can be written as

$$H^2 = \frac{8\pi G}{3} \rho_{m0} e^{-3x} + \alpha \left(\frac{1}{2} \frac{dH^2}{dx} + 2H^2 \right), \quad (23)$$

and this equation can be further rewritten as

$$E^2 = \Omega_{m0} e^{-3x} + \alpha \left(\frac{1}{2} \frac{dE^2}{dx} + 2E^2 \right), \quad (24)$$

where $E \equiv H/H_0$. Solving this equation, and using the initial condition $E_0 = E(t_0) = 1$, we have

$$E(z) = \left(\frac{2\Omega_{m0}}{2-\alpha}(1+z)^3 + \left(1 - \frac{2\Omega_{m0}}{2-\alpha}\right)(1+z)^{(4-\frac{2}{\alpha})} \right)^{1/2}. \quad (25)$$

There are also two model parameters, Ω_{m0} and α , in RDE model.

III. METHODOLOGY

A. Data analysis

In the following, we constrain the model parameters of these three DE models by using the latest observational data including the Union+CFA3 sample of 397 SNIa, the shift parameter of the CMB given by the five-year Wilkinson Microwave Anisotropy Probe (WMAP5) observations, and the baryon acoustic oscillation (BAO) measurement from the Sloan Digital Sky Survey (SDSS).

First, we consider the latest 397 Union+CFA3 SNIa data, the distance modulus $\mu_{obs}(z_i)$, compiled in Table 1 of [24]. This dataset add the CFA3 sample to the 307 Union sample [25]. The theoretical distance modulus is defined as

$$\mu_{th}(z_i) \equiv 5 \log_{10} D_L(z_i) + \mu_0, \quad (26)$$

where $\mu_0 \equiv 42.38 - 5 \log_{10} h$ with h the Hubble constant H_0 in units of 100 km/s/Mpc, and

$$D_L(z) = (1+z) \int_0^z \frac{dz'}{E(z'; \theta)} \quad (27)$$

is the Hubble-free luminosity distance $H_0 d_L$ (here d_L is the physical luminosity distance) in a spatially flat FRW universe, and here θ denotes the model parameters. The χ^2 for the SNIa data is

$$\chi_{SN}^2(\theta) = \sum_{i=1}^{397} \frac{[\mu_{obs}(z_i) - \mu_{th}(z_i)]^2}{\sigma_i^2}, \quad (28)$$

where $\mu_{obs}(z_i)$ and σ_i are the observed value and the corresponding 1σ error of distance modulus for each supernova, respectively. The parameter μ_0 is a nuisance parameter but it is independent of the data and the dataset. Following [26], the minimization with respect to μ_0 can be made trivially by expanding the χ^2 of Eq. (28) with respect to μ_0 as

$$\chi_{SN}^2(\theta) = A(\theta) - 2\mu_0 B(\theta) + \mu_0^2 C, \quad (29)$$

where

$$A(\theta) = \sum_{i=1}^{307} \frac{[\mu_{obs}(z_i) - \mu_{th}(z_i; \mu_0 = 0, \theta)]^2}{\sigma_i^2}, \quad (30)$$

$$B(\theta) = \sum_{i=1}^{307} \frac{\mu_{obs}(z_i) - \mu_{th}(z_i; \mu_0 = 0, \theta)}{\sigma_i^2}, \quad (31)$$

$$C = \sum_{i=1}^{307} \frac{1}{\sigma_i^2}. \quad (32)$$

Evidently, Eq. (28) has a minimum for $\mu_0 = B/C$ at

$$\tilde{\chi}_{SN}^2(\theta) = A(\theta) - \frac{B(\theta)^2}{C}. \quad (33)$$

Since $\chi_{SN,min}^2 = \tilde{\chi}_{SN,min}^2$, instead minimizing χ_{SN}^2 one can minimize $\tilde{\chi}_{SN}^2$ which is independent of the nuisance parameter μ_0 .

Next, we consider the constraints from CMB and LSS observations. For the CMB data, we use the CMB shift parameter R ; for the LSS data, we use the parameter A of the BAO measurement. It is widely believed that both R and A are nearly model-independent and contain essential information of the full CMB and LSS BAO data. The shift parameter R is given by [27, 28]

$$R \equiv \Omega_{m0}^{1/2} \int_0^{z_{rec}} \frac{dz'}{E(z')}, \quad (34)$$

where the redshift of recombination $z_{rec} = 1090$ [29]. The shift parameter R relates the angular diameter distance to the last scattering surface, the comoving size of the sound horizon at z_{rec} and the angular scale of the first acoustic peak in CMB power spectrum of temperature fluctuations [27, 28]. The measured value of R has been updated to be $R_{obs} = 1.710 \pm 0.019$ from WMAP5 [29]. The parameter A from the measurement of the BAO peak in the distribution of SDSS luminous red galaxies is defined as [30]

$$A \equiv \Omega_{m0}^{1/2} E(z_b)^{-1/3} \left[\frac{1}{z_b} \int_0^{z_b} \frac{dz'}{E(z')} \right]^{2/3}, \quad (35)$$

where $z_b = 0.35$. The SDSS BAO measurement [30] gives $A_{obs} = 0.469 (n_s/0.98)^{-0.35} \pm 0.017$, where the scalar spectral index is taken to be $n_s = 0.960$ as measured by WMAP5 [29]. Notice that both R and A are independent of H_0 , thus these quantities can provide robust constraint as complement to SNIa data on the holographic dark energy models. The total χ^2 is given by

$$\chi^2 = \tilde{\chi}_{SN}^2 + \chi_{CMB}^2 + \chi_{BAO}^2, \quad (36)$$

where $\tilde{\chi}_{SN}^2$ is given by Eq. (33), and the latter two terms are defined as

$$\chi_{CMB}^2 = \frac{(R - R_{obs})^2}{\sigma_R^2}, \quad (37)$$

and

$$\chi_{BAO}^2 = \frac{(A - A_{obs})^2}{\sigma_A^2}, \quad (38)$$

where the corresponding 1σ errors are $\sigma_R = 0.019$ and $\sigma_A = 0.017$, respectively. As usual, assuming the measurement errors are Gaussian, the likelihood function

$$\mathcal{L} \propto e^{-\chi^2/2}. \quad (39)$$

The model parameters yielding a minimal χ^2 and a maximal \mathcal{L} will be favored by the observations.

B. Model Comparison

For comparing different models, a statistical variable must be chosen. The χ_{min}^2 is the simplest one which is widely used. However, for models with different number of parameters, the comparison using χ^2 may not be fair, as one would expect that a model with more parameters tends to have a lower χ^2 . In this work, we will use the BE as a model selection criterion. The BE of a model M takes the form

$$\text{BE} = \int \mathcal{L}(\mathbf{d}|\theta, M) \mathbf{p}(\theta|M) d\theta, \quad (40)$$

where $\mathcal{L}(\mathbf{d}|\theta, M)$ is the likelihood function given by the model M and parameters θ (\mathbf{d} denotes the data), and $\mathbf{p}(\theta|M)$ is the priors of parameters. It is clear that a model favored by the observations should give a large BE. Since BE is the average of the likelihood of a model over its prior of the parameter space and automatically includes the penalties of the number of parameters and data, it is more reasonable and unambiguous than the χ_{min}^2 in model selection [31]. The logarithm of BE can be used as a guide for model comparison [31], and we choose the Λ CDM as the reference model: $\Delta \ln \text{BE} = \ln \text{BE}_{model} - \ln \text{BE}_{\Lambda\text{CDM}}$.

IV. RESULTS

We will show the results in this section. In Fig.1, we plot the contours of 68.3% and 95.4% confidence levels in the $\Omega_{m0} - c$ plane, for the HDE model. The best-fit model parameters are $\Omega_{m0} = 0.277$ and $c = 0.818$, corresponding to $\chi_{min}^2 = 465.912$. For 68.3% confidence level, $\Omega_{m0} = 0.277^{+0.022}_{-0.021}$, and $c = 0.818^{+0.113}_{-0.097}$; for 95.4% confidence level, $\Omega_{m0} = 0.277^{+0.037}_{-0.034}$, and $c = 0.818^{+0.196}_{-0.154}$.

In Fig.2, we plot the χ^2 and the corresponding likelihood \mathcal{L} of the ADE model. The best-fit model parameter is $n = 2.807$, giving $\chi_{min}^2 = 481.694$. For 68.3% confidence level, $n = 2.807^{+0.087}_{-0.086}$; for 95.4% confidence level, $n = 2.807^{+0.176}_{-0.170}$.

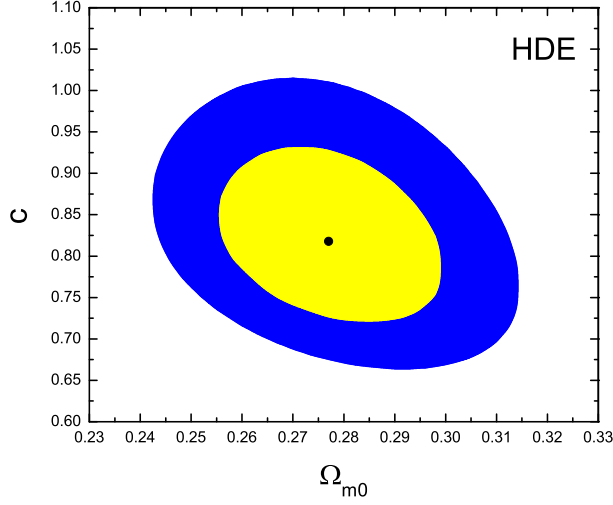


FIG. 1: Probability contours at 68.3% and 95.4% confidence levels in $\Omega_{m0} - c$ plane, for the HDE model. The round point denotes the best-fit values, $\Omega_{m0} = 0.277$ and $c = 0.818$, corresponding to $\chi^2_{min} = 465.912$.

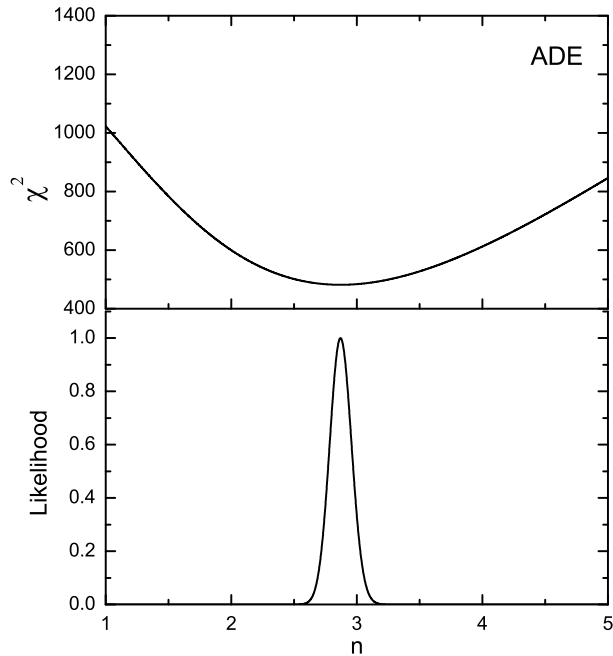


FIG. 2: The χ^2 and the corresponding likelihood \mathcal{L} of the ADE model.

In Fig.3, we plot the contours of 68.3% and 95.4% confidence levels in the $\Omega_{m0} - \alpha$ plane, for the RDE model. The best-fit model parameters are $\Omega_{m0} = 0.324$ and $\alpha = 0.371$, corresponding to $\chi^2_{min} = 483.130$. For 68.3% confidence level, $\Omega_{m0} = 0.324^{+0.024}_{-0.022}$, and $\alpha = 0.371^{+0.023}_{-0.023}$; for 95.4% confidence level, $\Omega_{m0} = 0.324^{+0.040}_{-0.036}$, and $\alpha = 0.371^{+0.037}_{-0.038}$.

Therefore, among these three holographic DE models, the HDE model can give the smallest χ^2_{min} . As a comparison, we also fit the Λ CDM model to the same observational data, and find that the minimal

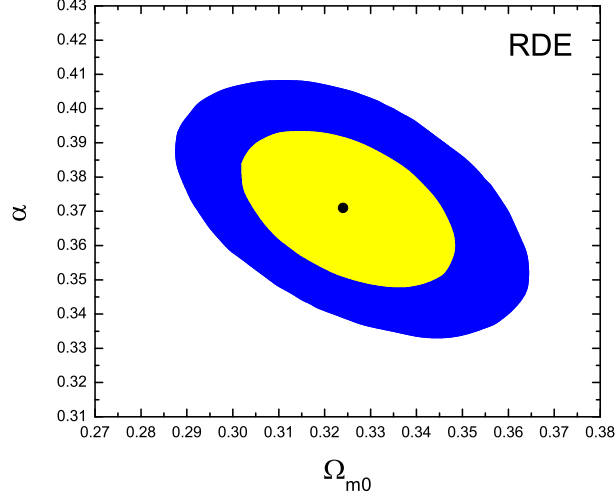


FIG. 3: Probability contours at 68.3% and 95.4% confidence levels in $\Omega_{m0} - \alpha$ plane, for the RDE model. The round point denotes the best-fit values, $\Omega_{m0} = 0.324$ and $\alpha = 0.371$, corresponding to $\chi^2_{min} = 483.130$.

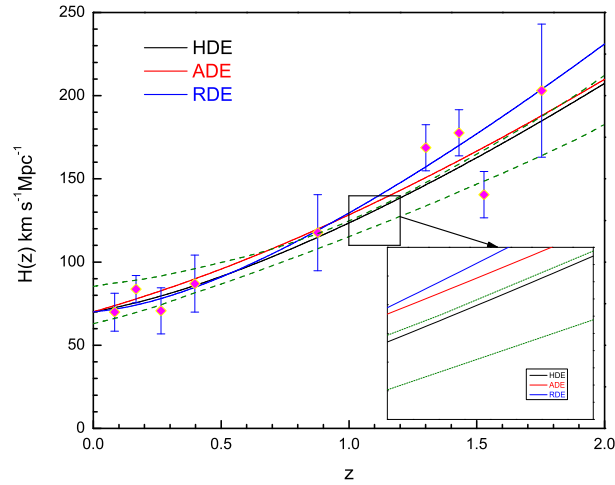


FIG. 4: Comparison of the observed $H(z)$, as square dots, with the predictions from the holographic DE models.

$\chi^2_{min} = 467.775$ for the best-fit parameter $\Omega_{m0} = 0.274$. Note that both HDE model and RDE model are two-parameter model, while ADE model is a single-parameter model. So, it is not suitable to choose the χ^2_{min} as a model selection criterion. In Table I, we list the results of $\Delta \ln BE$ for three holographic DE models. It is seen that although HDE model performs a little poorer than Λ CDM model, it performs better than ADE model and RDE model. Therefore, among these three holographic DE models, HDE is more favored by the observational data.

In Fig.4, we further compare the observed expansion rate $H(z)$ [32] with that predicted by these three holographic DE models (for each model, the best-fit values determined by SNIa+CMB+BAO analysis are taken). Notice that the area surrounded by two dashed lines shows the 68% confidence interval [2], and a

TABLE I: The results of $\Delta \ln \text{BE}$ for three holographic DE models.

Model	HDE	ADE	RDE
$\Delta \ln \text{BE}$	-0.86	-5.17	-8.14

DE model would be disfavored by the observation if it gives a curve of $H(z)$ that falls outside this area. It is seen that among these three holographic DE models, only the curve of $H(z)$ predicted by the HDE model falls inside this confidence interval. This result verifies our conclusion, from another perspective.

V. SUMMARY

In this work, we perform the best-fit analysis on three holographic DE models, by using the latest observational data including the Union+CFA3 sample of 397 SNIa, the shift parameter of the CMB given by the WMAP5 observations, and the BAO measurement from the SDSS. The analysis shows that for HDE, $\chi^2_{min} = 465.912$; for RDE, $\chi^2_{min} = 483.130$; for ADE, $\chi^2_{min} = 481.694$. Among these three DE models, the HDE model can give the smallest χ^2_{min} , which is even smaller than that given by the Λ CDM model. Moreover, we use the BE as a model selection criterion to make a comparison. Although HDE model performs a little poorer than Λ CDM model, it performs better than ADE model and RDE model. Therefore, among these three DE models, HDE is more favored by the observational data. Finally, adopting the best-fit values determined by SNIa+CMB+BAO analysis, we compare the observed expansion rate $H(z)$ with that predicted by these three holographic DE models. It is found that only the curve of $H(z)$ predicted by HDE model can fall inside the 68% confidence interval. This verifies our conclusion from another perspective.

It would be interesting to give tighter constrains on DE models by adding other cosmological observations, such as gamma-ray bursts [33], Chandra x-ray observation [34], and some old high-redshift objects [35]. This will be studied in a future work.

Acknowledgements

We would like to thank Hao Wei, Yan Gong, Chang-Jun Gao, and Feng-Quan Wu, for helpful discussions. This work is supported by the Natural Science Foundation of China.

-
- [1] A.G. Riess et al., *AJ*. **116**, 1009 (1998); S. Perlmutter et al., *ApJ* **517**, 565 (1999); J. L. Tonry et al., *ApJ* **594**, 1 (2003); R.A. Knop et al., *ApJ* **598**, 102 (2003); A.G. Riess et al., *ApJ* **607**, 665 (2004).
 - [2] C.L. Bennet et al., *ApJS*. 148, 1 (2003); D.N. Spergel et al., *ApJS*, 148, 175 (2003); D.N. Spergel et al., *ApJS* **170**, 377 (2007); L. Page et al., *ApJS* **170**, 335 (2007); G. Hinshaw et al., *ApJS* **170**, 263 (2007).
 - [3] M. Tegmark et al., *Phys. Rev.* **D69**, 103501 (2004); *ApJ* **606**, 702 (2004); *Phys. Rev.* **D74**, 123507 (2006).
 - [4] S. Weinberg, *Rev. Mod. Phys.* **61**, 1 (1989); arXiv:astro-ph/0005265; V. Sahni and A.A. Starobinsky, *Int. J. Mod. Phys. D* **9**, 373 (2000); S.M. Carroll, *Living Rev.Rel.* **4**, 1 (2001); P.J.E. Peebles and B. Ratra, *Rev. Mod. Phys.* **75**, 559 (2003); T. Padmanabhan, *Phys. Rept.* **380**, 235 (2003); E. J. Copeland, M. Sami and S. Tsujikawa, *Int. J. Mod. Phys. D* **15**, 1753 (2006).
 - [5] B. Ratra and P.J.E. Peebles, *Phys. Rev.* **D37**, 3406 (1988); P.J.E. Peebles and B.Ratra, *ApJ* **325**, L17 (1988); C. Wetterich, *Nucl. Phys.* **B302**, 668 (1988); I. Zlatev, L. Wang and P.J. Steinhardt, *Phys. Rev. Lett.* **82**, 896 (1999).
 - [6] R.R. Caldwell, *Phys. Lett. B* **545**, 23 (2002); S.M. Carroll, M. Hoffman and M. Trodden, *Phys. Rev.* **D68**, 023509 (2003).
 - [7] C. Armendariz-Picon, T. Damour and V. Mukhanov, *Phys. Lett. B* **458**, 209 (1999) ; C. Armendariz-Picon, V. Mukhanov and P.J. Steinhardt, *Phys. Rev.* **D63**, 103510 (2001); T. Chiba, T. Okabe and M. Yamaguchi, *Phys. Rev.* **D62**, 023511 (2000).
 - [8] T. Padmanabhan, *Phys. Rev.* **D66**, 021301 (2002); J.S. Bagla, H.K. Jassal, and T. Padmanabhan, *Phys. Rev.* **D67**, 063504 (2003).
 - [9] H. Wei, R.G. Cai, and D.F. Zeng, *Class. Quant. Grav.* **22**, 3189 (2005); H. Wei, and R.G. Cai, *Phys. Rev.* **D72**, 123507 (2005).
 - [10] A.Y. Kamenshchik, U. Moschella and V. Pasquier, *Phys. Lett. B* **511** 265 (2001); M.C. Bento, O. Bertolami and A.A. Sen, *Phys. Rev. D* **66** 043507 (2002); X. Zhang, F.Q. Wu and J. Zhang, *JCAP* **0601** 003 (2006).
 - [11] Y. Zhang, T.Y. Xia, and W. Zhao, *Class. Quant. Grav.* **24**, 3309 (2007); T.Y. Xia and Y. Zhang, *Phys. Lett. B* **656**, 19 (2007); S. Wang, Y. Zhang and T.Y. Xia, *JCAP* **10** 037 (2008).
 - [12] E. Witten, arXiv:hep-ph/0002297.
 - [13] G. 't Hooft, arXiv:gr-qc/9310026; L. Susskind, *J. Math. Phys.* **36** 6377 (1995).
 - [14] A.G. Cohen, D.B. Kaplan and A.E. Nelson, *Phys. Rev. Lett.* **82**, 4971 (1999).
 - [15] S.D.H. Hsu, *Phys. Lett. B* **594** 13 (2004).
 - [16] M. Li, *Phys. Lett. B* **603** 1 (2004).
 - [17] R.G. Cai, *Phys. Lett. B* **657**, 228 (2007).

- [18] H. Wei and R.G. Cai, *Phys. Lett. B* **660**, 113 (2008).
- [19] C. Gao, F.Q. Wu, X.L. Chen and Y.G. Shen, arXiv:0712.1394.
- [20] Q.G. Huang and M. Li, *JCAP* **0408**, 013 (2004); Q.G. Huang and M. Li, *JCAP* **0503**, 001 (2005); Q.G. Huang and Y.G. Gong, *JCAP* **0408**, 006 (2004); X. Zhang and F.Q. Wu, *Phys. Rev. D* **72**, 043524 (2005); X. Zhang, *Int. J. Mod. Phys. D* **14**, 1597 (2005); Z. Chang, F.Q. Wu and X. Zhang, *Phys. Lett. B* **633**, 14 (2006); B. Wang, E. Abdalla and R.K. Su, *Phys. Lett. B* **611**, 21 (2005); B. Wang, C.Y. Lin and E. Abdalla, *Phys. Lett. B* **637**, 357 (2006); X. Zhang, *Phys. Lett. B* **648**, 1 (2007); M.R. Setare, J. Zhang and X. Zhang, *JCAP* **0703**, 007 (2007); J. Zhang, X. Zhang and H. Liu, *Phys. Lett. B* **659**, 26 (2008); B. Chen, M. Li and Y. Wang, *Nucl. Phys. B* **774**, 256 (2007); J. Zhang, X. Zhang and H.Y. Liu, *Eur. Phys. J. C* **52**, 693 (2007); X. Zhang and F.Q. Wu, *Phys. Rev. D* **76**, 023502 (2007); C.J. Feng, *Phys. Lett. B* **633**, 367 (2008); Y.Z. Ma, Y. Gong and X.L. Chen, *Eur. Phys. J. C* **60**, 303 (2009); Y.Z. Ma, Y. Gong and X.L. Chen, arXiv:0901.1215; M. Li, C. Lin and Y. Wang, *JCAP* **0805**, 023 (2008); M. Li, X.D. Li, C. Lin and Y. Wang, *Commun. Theor. Phys.* **51**, 181 (2009); M. Jamil, M.U. Farooq and M.A. Rashid, *Eur. Phys. J. C* **61**, 471 (2009).
- [21] H. Wei and R.G. Cai, *Phys. Lett. B* **655**, 1 (2007); H. Wei and R.G. Cai, *Phys. Lett. B* **663**, 1 (2008); I.P. Neupane, *Phys. Rev. D* **76**, 123006 (2007); M. Maziashvili, *Phys. Lett. B* **666**, 364 (2008); J. Zhang, X. Zhang and H. Liu, *Eur. Phys. J. C* **54**, 303 (2008); J.P. Wu, D.Z. Ma and Y. Ling, *Phys. Lett. B* **663**, 152 (2008); H. Wei and R.G. Cai, *Eur. Phys. J. C* **59**, 99 (2009); J. Cui, L. Zhang, J. Zhang and X. Zhang, arXiv:0902.0716.
- [22] C.J. Feng, *Phys. Lett. B* **670**, 231 (2008); C.J. Feng, *Phys. Lett. B* **672**, 94 (2009); L.N. Granda and A. Oliveros, *Phys. Lett. B* **669**, 275 (2008); C.J. Feng, arXiv:0812.2067; K.Y. Kim, H.W. Lee and Y.S. Myung, arXiv:0812.4098; X. Zhang, arXiv:0901.2262; C.J. Feng and X. Zhang, arXiv:0904.0045; S. Nojiri and S.D. Odintsov, *Gen. Rel. Grav.* **38**, 1285 (2006).
- [23] R.G. Cai, B. Hu, and Y. Zhang, arXiv:0812.4504.
- [24] M. Hicken et al., arXiv:0901.4804.
- [25] M. Kowalski et al., *ApJ* **686**, 749 (2008).
- [26] S. Nesseris and L. Perivolaropoulos, *Phys. Rev. D* **72**, 123519 (2005); L. Perivolaropoulos, *Phys. Rev. D* **71**, 063503 (2005); S. Nesseris and L. Perivolaropoulos, *JCAP* **0702**, 025 (2007).
- [27] J.R. Bond, G. Efstathiou and M. Tegmark, *MNRAS*. **291**, L33 (1997).
- [28] Y. Wang and P. Mukherjee, *ApJ* **650**, 1 (2006).
- [29] E. Komatsu et al., *ApJS*. **180**, 3301 (2009).
- [30] D.J. Eisenstein et al., *ApJ* **633**, 560 (2005).
- [31] P. Mukherjee, D.R. Parkinson and A.R. Liddle, *ApJ* **638** L51 (2006); P. Mukherjee, D.R. Parkinson, P.S. Corasaniti, A.R. Liddle and M. Kunz, *MNRAS*. **369**, 1725 (2006); M. Kunz, R. Trotta and D. R. Parkinson, *Phys. Rev. D* **74**, 023503 (2006); A. R. Liddle, *MNRAS*. **377**, L74 (2007); R. Trotta, *MNRAS*. **378**, 72 (2007).
- [32] J. Simon, L. Verde, and R. Jimenez, *Phys. Rev. D* **71**, 123001 (2005).
- [33] Z.G. Dai, E.W. Liang and D. Xu, *ApJL*. **612**, 101 (2004); B.E. Schaefer, *ApJ* **660**, 16 (2007); Y. Wang, *Phys. Rev. D* **78**, 123532 (2008).
- [34] S.W. Allen, et al, *MNRAS*. **353**, 457 (2004); S.W. Allen, et al, *MNRAS*. **383**, 879 (2008).

- [35] A.C.S. Friacas, J.S. Alcaniz, and J.A.S. Lima, MNRAS. **362**, 1295 (2005); S. Wang and Y. Zhang, Phys. Lett. B **669** 201(2008).